

Binary PSO algorithm assisted to investigate the optical AND gate based- plasmonic nano- rods

M. AKHLAGHI*, F. EMAMI, N. NOZHAT

Opto-Electronic Department of Shiraz University of Technology, Shiraz, Iran

In this paper, a coherent perfect absorption (CPA)-type AND gate based on plasmonic nano particle is proposed. It consists of two plasmonic nano rod arrays on top of two serial arms with quartz substrate. The operation principle is based on the absorbable formation of a conductive path in the dielectric layer of a plasmonic nano-particles waveguide. Since the CPA efficiency depends strongly on the number of plasmonic nano-rod and the nano rod location, an efficient binary optimization method based the Particle Swarm Optimization (PSO) algorithm is used to design an optimized array of the plasmonic nano-rod in order to achieve the maximum absorption coefficient in the 'off' state and the minimum absorption coefficient in the 'on' state. In Binary PSO (BPSO), a group of birds consists a matrix with binary entries, control the presence ('1') or the absence ('0') of nano rod in the array.

(Received January 5, 2016; accepted November 25, 2016)

Keywords Plasmonic nano particles, Optimization algorithm, Optical gate

1. Introduction

The diffraction limit of light has been a fundamental obstacle for reducing the dimensions of optical logic components to the scales of electronic devices in integrated circuits [1, 2]. Plasmonic devices are well known for their ability to localize light beyond the diffraction limit [3–5]. Strong optical resonances can be designed by controlling the size and shape of the nanostructures in analogy to radio wave antennas. Therefore, some structures based on surface plasmon polaritons (SPPs), such as waveguides [6, 7], filters [8, 9], demultiplexers [10], modulators [11], reflector laser diodes [12], junctions [13], sensors [14, 15], and switches [16] have been proposed. In addition, some all optical logic gates, in nanophotonics plasmonics [17], with hybrid plasmonic-photonic crystal nano beam cavities [18], and based on waveguide type Kretschman Reather configuration on the metal surface [19] have been proposed and analyzed. Also, some other logic gates based on silicon micro-ring resonators [20], two photon absorption in silicon waveguides [21], cross phase modulation [22], and single semiconductor optical amplifiers have been investigated [23]. Some of these devices employ the effects of electro-optic or magneto-optic by applying respectively an electric or magnetic field, which has some disadvantages in switching time, loss and size [24, 25]. Design and implementation of more complex logic gates can be accomplished by combining and cascading these logic gates appropriately. Their performances can be adjusted by variation of the structural parameters to achieve desired operations. Plasmonic logic gates can highly reduce the sizes and hence the signal losses, decrease the signal thresholds for the logic operations, and can provide fast switching optical devices. The optimization problems in the plasmonic nano-

structure area can be divided into two categories. In the first type the continuous optimization algorithm can be performed to engineer the geometrical metal nano-structures [26], whereas in the second type, the binary optimization algorithm can be used to control the presence ('1') or absence ('0') of the metal nano particles in the array [27]. In ref [28], binary TLBO algorithm was used and an optical switch based on the dimer plasmonic nano-rods has been proposed. In this paper BPSO algorithm is used to control the existence ('1') or non-existence ('0') of plasmonic nano particles to design an optical AND gate. In BPSO, a swarm consists of a matrix with binary entries control the presence ('1') or the absence ('0') of nano single nano-rod in the array and find the best array of nano-rod from all possible arrays. The selected array should be able to maximize the absorption coefficient in the "off" state and minimize the absorption coefficient in the "on" state.

2. Model description

The proposed plasmonic AND gate has been shown schematically in the figure 1. Here, the feasibility of the plasmonic optical AND gate has been investigated by integrating the coherent perfect absorption (CPA) devices into integrated photonic waveguides. In this figure, the plasmonic AND gate has two serial arms and any arm consists of an array of metallic nano rod. In any arm, the integrated plasmonic waveguides has been excited by two monochromatic incident plan-waves with the same frequency and two angles of incident $\theta=0$ (pump Input) and $\theta=90$ (Input A or Input B). When only the signal with $\theta=0$ is applied, coherent perfect absorption (CPA) occurs and the incident wave is suppressed whereas when both signals are applied to the plasmonic waveguide

simultaneously ($\theta=0$ and $\theta=90$), the absorption suppresses and two incident waves are transmitted from output. Therefore, the signal with $\theta=90$ acts as control signal. Depends on whether control signal is lunched into the waveguide or not, the absorption can be suppressed or maximized. In figure.1, when input A and input B are applied, the absorption suppressed in both arms and pump input transmits from the first and second arms, therefore appear in output ($A=1, B=1, \text{output}=1$). When Input A is

applied and Input B is zero, the pump transmits from the first arm, but suppresses in the second arm, ($A=1, B=0, \text{output}=0$). When Input A is zero and Input B is applied to the waveguide the pump suppresses in the first arm, therefore output is zero ($A=0, B=1, \text{output}=0$) while when both inputs are zero, the CPA occurs for both arm and pump input strongly suppresses, therefore output is zero ($A=0, B=0, \text{output}=0$). This procedure is shown schematically in Fig. 2.

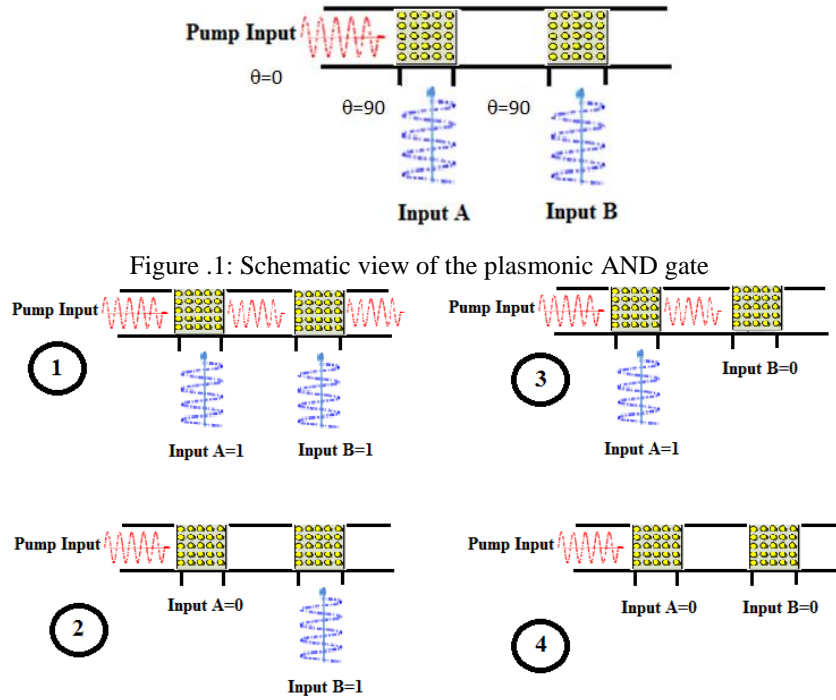


Figure .1: Schematic view of the plasmonic AND gate

Fig. 2. Schematic view of the procedure of plasmonic nano rod AND gate 1) $A=1, B=1, \text{output}=1$
2) $A=0, B=1, \text{output}=0$ 3) $A=1, B=0, \text{output}=0$ 4) $A=0, B=0, \text{output}=0$

3. Background of Numerical Method

The wide range of applications and exploitation possibilities of optical plasmonic properties of metals demand numerical techniques which provide accurate modeling and analysis of problems involving metal-dielectric interfaces in visible and near-infrared bands. Since optical response of metals can be well-described in the classical framework based on Maxwell's equations [29], differential formulations as the finite difference time domain (FDTD) [30] or the finite integration technique [31] have been commonly used to solve this kind of problems due to their easy implementation from differential equations. Mainly due to the high computational requirements of the differential techniques, alternative tools demanding a lower number of unknowns for a given problem such as surface integral equation (SIE) formulations solved by the well-known method of moments (MoM) [31] have increased their presence in the context of plasmonics [32–34]. Moreover, there are some numerical simulation methods to study the interaction between the light and metal nano particles such as FDTD [35], FEM (Finite Element Method) [36], DDA (Discrete-

dipole Approximation) [37], Mie Theory [38] and Transition matrix (T-matrix) theory [38]. In this paper, DDA is used to study the optical properties of plasmonic nano particles.

4. Theory

The plasmonic AND gate, depicted in Figure 1, consists of two arrays of metallic nano rod that are periodically arranged in the $x y$ -plane of the quartz substrate. The device is excited by a monochromatic incident plan wave $\mathbf{E}_{inc}(r, t) = \mathbf{E}_0 e^{j(kr - \omega t)}$ where $r, t, \omega, k = \omega/c = 2\pi/\lambda, c,$ and λ are the position vector, the time, the angular frequency, the wave vector, the speed of light, and the wavelength of the incident light, respectively. To calculate the E-field of each dipole, time harmonic component $-j\omega t$ of the E-field is left out. Local field arises from the incident light with polar (θ) and azimuth (ϕ) angles at each particle are:

$$\mathbf{E}_{inc}(\mathbf{r}_s) = \mathbf{E}_0 e^{j\mathbf{k}\cdot\mathbf{r}_s} \quad (1)$$

Where

$$\mathbf{k} = \frac{2\pi}{\lambda} [\sin(\theta) \cdot \cos(\varphi), \sin(\theta) \cdot \sin(\varphi), \cos(\theta)] \quad (2)$$

For the incident field with P-polarization:

$$\mathbf{E}_0 = [\sin(\theta - \frac{\pi}{2}) \cdot \cos(\varphi), \sin(\theta - \frac{\pi}{2}) \cdot \sin(\varphi), \cos(\theta - \frac{\pi}{2})] \quad (3)$$

and for the incident field with S-polarization:

$$\mathbf{E}_0 = [\cos(\varphi + \frac{\pi}{2}), \sin(\varphi + \frac{\pi}{2}), 0] \quad (4)$$

When the applied field is parallel to one of the principle axes, the polarizability, α , is given by [39]:

$$\alpha = V \epsilon_0 \frac{\epsilon_r - 1}{1 + L_1 (\epsilon_r - 1)} \quad (5)$$

where $\epsilon_r = \epsilon_{particle} / \epsilon_{medium}$ is the relative dielectric function of the particle with respect to the medium, V is the particle volume, and L_1 is the shape factor. The exact equation for L_1 is given by [28]:

$$L_1 = \frac{1}{AR^2 - 1} \left(\frac{AR}{2(AR^2 - 1)^{\frac{1}{2}}} \cdot \text{Ln} \left(\frac{AR + (AR^2 - 1)^{\frac{1}{2}}}{AR - (AR^2 - 1)^{\frac{1}{2}}} \right) - 1 \right) \quad (6)$$

where AR is aspect ratio. The gold nano rods with different aspect ratio $AR = H/D$, width D , height H , arc factor L , and the eccentricity $e = 2L/D$ are shown in Figure 3. In this figure the perfect cylinder and cylinder with two semi-spherical end caps simulated under $e = 0$ and $e=1$ condition, respectively.

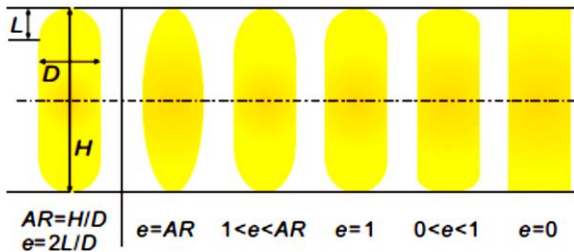


Fig. 3. Geometric characterization of the plasmonic nano rod with different e , D , and AR [28].

The dipole moment induced in a single particle by a local electric field is given by:

$$\mathbf{P}_s = \epsilon_0 \alpha_s \mathbf{E}_{Loc}(\mathbf{r}_s) \quad (7)$$

Here, \mathbf{P}_s is the induced dipole moment, α_s is Polarizability of the particle centered at \mathbf{r}_s , \mathbf{E}_{Loc} is local electric field, and ϵ_0 is permittivity of free space. The local field arises from two sources, appearing as two terms. The first term is incident light, $\mathbf{E}_{inc}(\mathbf{r}_s) = \mathbf{E}_0 e^{j\mathbf{k} \cdot \mathbf{r}_s}$, and the field radiated from each of the other $N-1$ radiating dipoles in the array. Combining these terms leads to local field at each dipole as follow [40]:

$$\mathbf{E}_{loc,i} = \mathbf{E}_{inc,i} + \mathbf{E}_{dip,i} = \mathbf{E}_0 e^{j\mathbf{k} \cdot \mathbf{r}_i} - \sum_{i \neq j} \mathbf{A}_{i,j} \mathbf{P}_j \quad (8)$$

where \mathbf{P}_s is the dipole moment of the s -th particle and $\mathbf{A}_{s,h}$ with $s \neq h$ is an interaction matrix with $3N \times 3N$ matrixes as elements described by following equation [40]:

$$\mathbf{A}_{ij} = \frac{e^{ikr_{ij}}}{r_{ij}^3} \left\{ k^2 r_{ij} \times (r_{ij} \times \mathbf{P}_j) + \frac{(1 - ikr_{ij})}{r_{ij}^2} [r_{ij}^2 \mathbf{P}_j - 3r_{ij} (r_{ij} \cdot \mathbf{P}_j)] \right\} \quad (9)$$

where $\mathbf{r}_{s,h} = \mathbf{r}_s - \mathbf{r}_h$, $r_{sh} = |\mathbf{r}_{sh}|$ and $\mathbf{A}_{s,h}$ are 3×3 matrices representing the interaction of two particles of s and h . Once the $3N$ -coupled complex linear equations, given by Eq. 9, are solved and each dipole moment \mathbf{P}_i determined, and the optical absorption can be directly calculated from the dipole array as follow [40]:

$$Q_{abs} = \frac{4\pi k}{|\mathbf{E}_0|^2 \pi \alpha^2} \sum_{i=1}^N \left\{ \text{Im}[\mathbf{P}_i (\alpha_i^{-1})^* \mathbf{P}_i^* - \frac{2}{3} k^3 |\mathbf{P}_i|^2] \right\} \quad (10)$$

4.1. Binary Particle Swarm Optimization Algorithm

The PSO algorithm is an optimization procedure inspired by a colony such as birds which can improve its behaviors [23]. Any element of this colony is called a particle and moves in an n -dimensional space, correcting its trajectory based on the previous actions of itself and its neighboring particles. For each particle, velocity and displacement are updated based on the following relations [41]:

$$v_i^{k+1} = w v_i^k + c_1 r_1 (p_i^k - x_i^k) + c_2 r_2 (p_g^k - x_i^k) \quad (11)$$

$$x_i^{k+1} = x_i^k + v_i^{k+1}, \quad i = 1, \dots, n \quad (12)$$

where k is the number of the current iteration, n is the number of particles, w is the inertia weight, c_1 and c_2 are acceleration parameters, and finally r_1 and r_2 are random parameters between 0 and 1. The best position for the i -th particle which has been stored so far is represented as [42]:

$$\mathbf{P}_i^k = [p_1^k, p_i^k, \dots, p_n^k]^T \quad (13)$$

All the \mathbf{P}_i^k (p_best) are evaluated by a fitness function. The best particle among all p_best is represented as \mathbf{P}_g^k ($Gbest_best_value$), which in a minimization problem \mathbf{P}_g^k is the smallest member of the \mathbf{P}_i^k vector while for a maximization problem it is the largest member of \mathbf{P}_i^k . PSO was designed for continuous problems, but cannot deal with discrete problems. A new version of PSO, called Binary PSO (BPSO), was introduced by Kennedy and Eberhart in 1997 and applied to discrete binary variables. After that, many optimization problems in various areas were solved by this method. The position in BPSO is represented by a binary vector and the velocity is still a floating-point vector; however, velocity is used to determine whether the probability changes from 0 to 1 or from 1 to 0 when the positions of particles are being updated. The equation for updating the positions is then replaced with [43-45]:

$$sigmoid(v_{id}^k) = \frac{1}{1 + e^{(-v_{id}^k)}} \quad (14)$$

$$x_{id}^k = \begin{cases} 1, & \text{if } rand < sigmoid(v_{id}^k) \\ 0 & \text{otherwise} \end{cases} \quad (15)$$

Since the CPA depends strongly on the number of plasmonic nano-rod and the nano-rod location, BPSO algorithm has been used to control the presence ('1') or the absence ('0') of nano rod in the array and find the best array of plasmonic nano-rod from all possible arrays. In order to increase the CPA efficiency, the selected array should be able to maximize the absorption coefficient in "off" state and minimize the absorption coefficient in "on" state.

5. Simulation results

Consider a quartz substrate with 25 plasmonic nano-rods (5×5). There is a 25nm gap between metallic nano-rod. In this simulation we assumed that nano rod have 10 nm diameters and 12 nm height with L=0. To find the absorption coefficient, we used the DDA method described in theory section. Fig. 4 shows the absorption spectrum across the entire interval 200–600 nm in two cases. In the first case, only the signal with $\theta=0$ is entered into the waveguide, whereas in the second case, two signals with the same frequency and two directions $\theta=0$ and $\theta=90$ are entered in the optical waveguide. When only the signal with $\theta=0$ is applied, coherent perfect absorption (CPA) occurs and the incident waves is suppressed for $\lambda=220\text{nm}$ and when both signals are applied to the

waveguide, absorption is suppresses and the two incident waves are transmitted for $\lambda=220\text{nm}$. In this figure, the dash line shows the absorption coefficient in the "off" state and the bold line is the absorption coefficient in the "on" state. Since the CPA depends strongly on the number of plasmonic nano-rod and the nano rod location, our goal is to control the presence ('1') or the absence ('0') of metallic nano rod in the array and find the best array of single nano rod from all possible arrays. The selected array should be able to maximize the absorption coefficient in the "off" state and minimize the absorption coefficient in the "on" state. On other words the goal is to minimize the Q_{abs} when two signals with two directions are entered and maximize the absorption coefficient when one signal is entered by optimizing 25 binary nano rod for 2D arrays (5×5). As seen, BPSO is an algorithm that minimizes a profit function. To use BPSO algorithm for maximizing absorption coefficient, BPSO method should be minimized the following function:

$$Cost\ function = -(Q_{1abs}(\lambda_i) - Q_{2abs}(\lambda_i)) \quad (16)$$

Where λ_i is a specific wavelength in which the optimization is carried out, Q_{1abs} is the absorption coefficient in "off" state and Q_{2abs} is the absorption coefficient in "on" state. Optimization algorithm is applied and controls the presence "1" or the absence of metallic nano rod in order to engineering the absorption coefficient to design an optical AND gate. Figure 5 shows the absorption spectra of the optimized array (5*5) in which the optimization is perform around $\lambda_i=510\text{nm}$. Moreover, the dash line shows the absorption coefficient when one signal is lunched to the waveguide and the bold line is the absorption coefficient when two signals are lunched in the waveguide. As shown in this figure, metallic nano rod with this layout has high absorption in the 'off' state and low absorption in the 'on' state. The main feature of interest in view of the current work is the resonant behavior of optimized metallic nano-rod under the excitation of an external EM radiation, which leads to a very strong amplification of the EM fields inside and in the near field range outside the particles. Correspondingly, such systems exhibit strong resonance peaks in the absorption of light, whose characteristics (position and line width) depend on both intrinsic geometrical factors (single-particle size and shape) and extrinsic parameters (dielectric constant of the host, proximity of a surface or other polarizable entities). Such features, not observed in the bulk counterparts, are a characteristic effect of the collective oscillations of the electrons gas confined inside the metallic structures, and are given the name of localized surface plasmon resonances. In figure 5, BPSO was used to control the presence or the absence of plasmonic nano particles to have strong resonance peaks in the absorption of light when two signals are entered and low resonance peaks in the absorption of light when one signal is entered. Depending on the position and number of the plasmonic nano rod, local field of each nano particle minimized or maximized. Therefore according to equation 10 the absorption can be suppressed for one wavelength and

maximized for the other wavelength. The splitting and broadening of the single-particle resonances are determined by the strength of the interactions between adjacent particles, and they can be tuned by varying the separation or the number of the particles forming the chain. The interaction between nine nano-rods in figure 5 creates new LSP resonances which are a result of the coupling between the various individual LSP resonances of the isolated particles. Additionally, since plasmon waves couple strongly only in the near-field regime at very short distances, closely packed clusters is also needed in order to achieve high field enhancement.

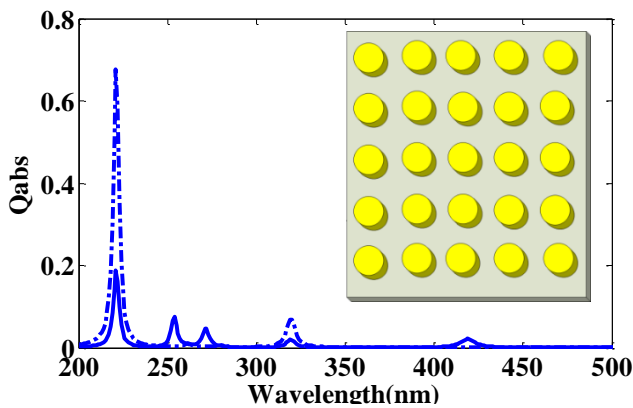


Fig. 4. Absorption coefficient of periodic plasmonic nano rod.

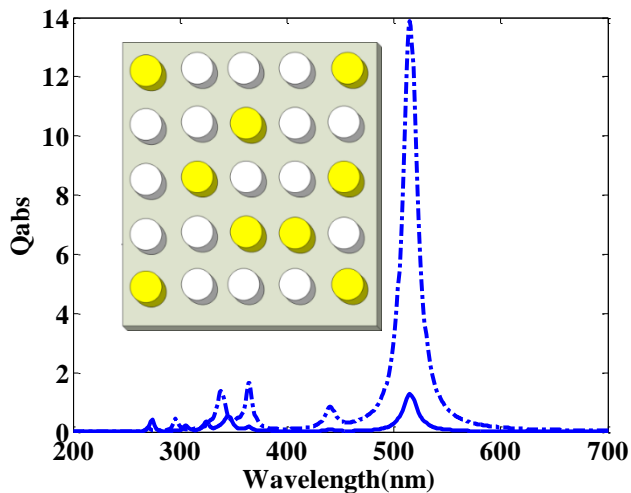


Fig. 5. Absorption coefficient of optimized plasmonic nano rod in which optimization perform around $\lambda_i=510\text{nm}$

6. Conclusion

We have utilized an ultra-small plasmonic nano rod to induce coherent perfect absorption (CPA) in the quartz waveguide in order to develop an optical AND gate. Since CPA effect can be improved with optimize selection of gold nano rod layout, the BPSO is proposed to design an array of plasmonic nano rod in order to achieve maximum absorption coefficient in the “off” state and lower absorption coefficient in the “on” state.

References

- [1] S. A. Maier, M. L. Brongersma, P. G. Kik, S. Meltzer, A. G. Requicha, H. A. Atwater, *Adv. Mater.* **13**, 1501 (2001).
- [2] P. Tuchscherer, *Opt. Express* **17**, 14235 (2009).
- [3] V. Giannini, A. I. Fernández-Domínguez, Y. Sonnefraud, T. Roschuk, R. Fernández-García, S. A. Maier, *Small* **6**(22), 2498 (2010).
- [4] J. A. Schuller, E. S. Barnard, W. Cai, Y. C. Jun, J. S. White, M. L. Brongersma, *Nat. Mater.* **9**(3), 193 (2010).
- [5] D. K. Gramotnev, S. I. Bozhevolnyi, *Nat. Photonics* **4**(2), 83 (2010).
- [6] J. Jung, *J. Opt. Soc. Korea* **14**, 277 (2010).
- [7] B. Jafarian, N. Nozhat, N. Granpayeh, *J. Opt. Soc. Korea* **15**, 118 (2011).
- [8] H. Lu, X. Liu, Y. Gong, L. Wang, D. Mao, *Opt. Commun.* **284**, 2613 (2011).
- [9] A. Setayesh, S. R. Mirnaziry, M. S. Abrishamian, *J. Opt. Soc. Korea* **15**, 82 (2011).
- [10] G. Wang, H. Lu, X. Liu, D. Mao, L. Duan, *Opt. Express* **19**, 3513 (2011).
- [11] Z. Lu, W. Zhao, *J. Opt. Soc. Am. B* **29**, 1490 (2012).
- [12] S. Kim, Y. T. Byun, D. G. Kim, N. Dagli, Y. Chung, *J. Opt. Soc. Korea* **14**, 38 (2010).
- [13] M. Farahani, N. Granpayeh, M. Rezvani, *J. Opt. Soc. Am. B* **29**, 1722 (2012).
- [14] J. H. Jung, M. W. Kim, *J. Opt. Soc. Korea* **11**, 55 (2007).
- [15] K. M. Byun, *J. Opt. Soc. Korea* **14**, 65 (2010).
- [16] H. Lu, X. Liu, L. Wang, Y. Gong, D. Mao, *Opt. Express* **19**, 2910 (2011).
- [17] H. Wei, Z. Wang, X. Tian, M. Kall, H. Xu, *Nature Commun.* **1388**, 1 (2011).
- [18] I. S. Maksymov, *Phys. Lett. A* **375**, 819 (2011).
- [19] G. Y. Oh, D. G. Kim, Y. W. Choi, “All-optical logic gate using waveguide-type SPR with Au/ZnO plasmon stack,” in *Proc. Opto Electron. and Commun. Conference (Japan, 2010)*, pp. 374-375.
- [20] Q. Xu, M. Lisbon, *Opt. Express* **15**, 924 (2007).
- [21] T. K. Liang, L. R. Numes, M. Tsuchiya, K. S. Abedin, T. Miyazaki, D. V. Thourhout, W. Bogaetrs, P. Dumon, R. Baets, H. K. Tsang, *Opt. Commun.* **256**, 171 (2006).
- [22] J. H. Kim, B. K. Kang, Y. H. Park, Y. T. Byun, S. Lee, D. H. Woo, S. H. Kim, *J. Opt. Soc. Korea* **5**, 25 (2001).
- [23] S. Kaur, R. S. Kaler, *J. Opt. Soc. Korea* **16**, 13 (2012).
- [24] T. Yabu, M. Geshibo, T. Kitamura, K. Nishida, S. Sawa, *IEEE J. Quantum Electron.* **38**, 37 (2009).
- [25] Y. H. Pramono and Endarko, *J. Nonlin. Opt. Phys. and Mater.* **10**, 209 (2001).
- [26] M. Akhlaghi, F. Emami, N. Nozhat, *Optoelectron. Adv. Mat.* **8**(9-10), 845 (2014).
- [27] M. Akhlaghi, F. Emami, N. Nozhat, *Modern Opt.* **61**(13), 1092 (2014).
- [28] M. Akhlaghi, N. Nozhat, F. Emami, *IEEE Transaction on Nanotechnology*, **13**(6), 1172 (2014).

- [29] A. Taflove, M. E. Brodwin, *IEEE Trans. Microw. Theory Tech.* **23**(8), 623 (1975).
- [30] T. Weiland, *Arch. Elektron. Übertragungstech.* **31**, 116 (1977).
- [31] R. F. Harrington, *Field Computation by Moment Method* (IEEE Press, 1993).
- [32] A. M. Kern, O. J. F. Martin, *J. Opt. Soc. Am. A* **26**(4), 732 (2009).
- [33] B. Gallinet, A. M. Kern, O. J. F. Martin, *J. Opt. Soc. Am. A* **27**(10), 2261 (2010).
- [34] J. M. Taboada, J. Rivero, F. Obelleiro, M. G. Araújo, L. Landesa, *J. Opt. Soc. Am. A* **28**(7), 1341 (2011).
- [35] A. Taflove, S. C. Hagness, "Computational Electrodynamics: The Finite Difference Time Domain Method," second edition, Artech House, ANDwood, MA, 2000.
- [36] J.M. Jin, *The Finite Element Method in Electromagnetics*, 2nd edition, New York: John Wiley & Sons, 2002.
- [37] B.T. Draine, P.J. Flatau, *J. Opt. Soc. Am. A* **11**, 1491 (1994).
- [38] C. Forestiere, G. Miano, S. V. Boriskina, L. D. Negro, *Opt. Express* **17**, 9648 (2009).
- [39] C.F Bohren, D.R Huffman, "Absorption and Scattering of Light by Small Particles", John Wiley and Sons, (1998).
- [40] L.Y. Loke, M. P. Mengüç, T. A. Nieminen, *Journal of Quantitative Spectroscopy and Radiative Transfer*, **112**(11), 1711 (2011).
- [41] F. Emami, M. Akhlaghi, *J. Photonics Technology letters* **24**, 1349 (2012).
- [42] M. Akhlaghi, F. Emami, *J. Opt. Soc. Korea* **17**, 237 (2013).
- [43] Akhlaghi, Majid, Farzin Emami, Najmeh Nozhat. *Optical and Quantum Electronics* **47**(7), 1713 (2015).
- [44] Akhlaghi, Majid, Rasul Keshavarzi, Farzin Emami, *Optical and Quantum Electronics* **47**(8), 2605 (2015).
- [45] Emami, Farzin, Majid Akhlaghi, Najmeh Nozhat. *Journal of Computational Electronics* **14**(2), 574 (2015).

*Corresponding author: m.akhlaghi@sutech.ac.ir